

Laser confocal endomicroscopy as a novel technique for fluorescence diagnostic imaging of the oral cavity

Patricia Soo-Ping Thong

Malini Olivo

Kiang-Wei Kho

Wei Zheng

National Cancer Center
Division of Medical Sciences
11 Hospital Drive
Singapore, Singapore 169610

Kent Mancner

Changi General Hospital
Laboratory Medicine Service
2 Simei Street 3
Singapore, Singapore 529889

Martin Harris

Optiscan Pty. Ltd.
Department of Fundamental Research
15-17 Normanby Road
Melbourne 3168 Australia

Khee-Chee Soo

National Cancer Center
Division of Medical Sciences
11 Hospital Drive
Singapore 169610
and
Singapore General Hospital
Department of Surgery
Outram Road
Singapore, Singapore 169608

Abstract. Malignancies of the oral cavity are conventionally diagnosed by white light endoscopy, biopsy, and histopathology. However, it is often difficult to distinguish between benign and premalignant or early lesions. A laser confocal endomicroscope (LCE) offers noninvasive, *in vivo* surface and subsurface fluorescence imaging of tissue. We investigate the use of an LCE with a rigid probe for diagnostic imaging of the oral cavity. Fluorescein and 5-aminolevulinic acid (ALA) were used to carry out fluorescence imaging *in vivo* and on resected tissue samples of the oral cavity. In human subjects, ALA-induced protoporphyrin IX (PpIX) fluorescence images from the normal tongue were compared to images obtained from patients with squamous cell carcinoma (SCC) of the tongue. Using rat models, images from normal rat tongues were compared to those from carcinogen-induced models of SCC. Good structural images of the oral cavity were obtained using ALA and fluorescein, and morphological differences between normal and lesion tissue can be distinguished. The use of a pharmaceutical-grade solvent Pharmasolve® enhanced the subsurface depth from which images can be obtained. Our initial results show that laser confocal fluorescence endomicroscopy has potential as a noninvasive optical imaging method for the diagnosis of oral cavity malignancies. © 2007 Society of Photo-Optical Instrumentation Engineers. [DOI: 10.1117/1.2710193]

Keywords: laser confocal endomicroscopy; fluorescence diagnostic imaging; oral cavity; 5-aminolevulinic acid (ALA); protoporphyrin IX (PpIX) fluorescence; fluorescein.

Paper 05343RR received Nov. 16, 2005; revised manuscript received Nov. 3, 2006; accepted for publication Nov. 9, 2006; published online Mar. 1, 2007.

1 Introduction

The predominant type of cancer of the oral cavity is squamous cell carcinoma (SCC). Globally, cancers of the mouth and pharynx rank sixth overall.¹ The major risk factor for oral cancer is the use of tobacco, including smoking tobacco, chewing betel nut, and the use of snuff.² Early detection is crucial for a good prognosis. The conventional approach for diagnosis of oral cavity malignancies is to use white light endoscopy followed by histopathological examination of biopsies of suspicious-looking tissue. However, early oral cavity lesions are often flat or superficial, and it is difficult to distinguish between benign and premalignant or early lesions. Histopathological examination of biopsy tissue remains the gold standard for definitive diagnosis. Biopsy samples of tissue are collected and processed in a specialist laboratory, where a medically trained staff reviews the results to determine whether there are any tissue abnormalities. This process is time consuming, and while the biopsy procedure is generally safe, there are risks of complications for the patients arising

from the biopsy procedure. In addition, histopathology has its limitations (small size and inadequate depth of specimen, sampling artifacts such as crushing of tissue and heat artifact) and is dependent on the skill of the operator as well as the observer. Histopathology is evaluation at one moment in time. Observation that is noninvasive can monitor changes in morphology. Hence there is a need to develop a more definitive, noninvasive, *in vivo* diagnostic technique for the early diagnosis of malignancies in the oral cavity.

Laser confocal endomicroscopy is a noninvasive endoscopic technique that offers *in vivo* surface and subsurface optical imaging of tissue at the cellular level.^{3,4} It can be used with a fluorescent dye to carry out fluorescence microscopic imaging of tissue. In recent years, a laser confocal endomicroscope (LCE) with a flexible endoscope has been developed for diagnostic imaging of the upper and lower gastrointestinal tract.⁵⁻⁷ However, such systems are not suitable for imaging the oral cavity. In this pilot study, we investigated the use of a prototype LCE with a rigid probe for diagnostic imaging of the oral cavity.

Address all correspondence to Malini Olivo, National Cancer Center, Division of Medical Sciences, 11 Hospital Drive, Singapore 169610; Tel: 65 64368317; Fax: 65 63720161; E-mail: dmsmcd@nccs.com.sg

The nonfluorescent compound 5-aminolevulinic acid (ALA) is an endogenous metabolite involved in the haeme production pathway. It is a precursor of the fluorescent metabolite protoporphyrin IX (PpIX). Exogenous application of ALA results in the increased production and preferential accumulation of PpIX in tumour tissue.⁸ Several research groups, including ours, have investigated the use of ALA in macroscopic fluorescence diagnostic endoscopy of cancer. Results show that endoscopic imaging of ALA-induced PpIX fluorescence at the macroscopic level is superior to white light endoscopy as a diagnostic tool for the detection of various types of cancers, including those in the oral cavity.^{9–13} In a preliminary study, we have shown that laser confocal endomicroscopy holds promise for rapid, noninvasive diagnosis of oral cavity malignancies at the microscopic level.¹⁴ In this follow-up study, we further investigated ALA-induced PpIX fluorescence endomicroscopic imaging as a technique for fluorescence diagnostic imaging of the oral cavity in both human and animal subjects.

An LCE with a handheld rigid probe was used to capture ALA-induced PpIX fluorescence images of the normal human tongue in healthy volunteers and compared to images obtained from patients with SCC of the tongue. Using animal models, rat oral cavity images obtained from ALA-induced PpIX fluorescence were compared to images obtained using fluorescein sodium, a contrast agent that is commonly used for fluorescence imaging. Fluorescence images obtained using the LCE with ALA and fluorescein were compared to those obtainable using a conventional benchtop confocal laser scanning microscope (CLSM). A carcinogen-induced model of oral cavity SCC, a 4-nitroquinoline N-oxide (4-NQO)-induced SCC rat model, was used for comparison between a healthy rat tongue and an SCC rat tongue. To enhance drug penetration and increase the subsurface depth from which images can be obtained, we also investigated the efficacy of using Pharmasolve (N-methyl-pyrrolidone), a pharmaceutical-grade solvent, together with ALA and fluorescein in animal models. Pharmasolve is known to enhance bioavailability of topical formulations by enhancing penetration in tissue.¹⁵ ALA-induced PpIX and fluorescein fluorescence images of the normal rat oral cavity were compared to images obtained from 4-NQO-induced SCC models.

2 Materials and Methods

2.1 Instrumentation

Figure 1 shows the schematic diagram of the prototype LCE system developed by Optiscan Imaging Ltd. (Victoria, Australia) for *in vivo* fluorescence imaging of human tissue. A band-pass filter in front of the argon ion (Ar^+) laser selectively passes the 488-nm wavelengths while rejecting all plasma emissions. The selected 488-nm laser beam then passes through a beamsplitter and is focused into a single-mode fiber via two reflecting mirrors and a focusing lens. The beamsplitter also serves as a reflecting mirror for the return fluorescence signal and directs it to a photomultiplier tube (PMT) via a mirror, as shown in the diagram. A high-rejection 505-nm long-pass filter further absorbs the backscattered laser beam while transmitting the fluorescence signal to a sensitive PMT for detection.

The handheld rigid probe consists of a handle with a focusing knob and an 8-mm (\varnothing) metal tube (see inset) that houses a miniaturized tuning fork. The output end of the single-mode fiber is attached to one of the arms of the tuning fork. A driving magnetic coil induces a 700-Hz resonant oscillation in the tuning fork, providing a fast *x* scan, while a second coil causes the entire tuning fork to pivot in the *y* direction at a slower scanning rate of 1 to 2 Hz. An objective lens is used both to focus the excitation laser into the tissue as well as to collect the fluorescence signal. These give a maximum imaging area of approximately $390\ \mu\text{m} \times 390\ \mu\text{m}$. Due to the small size of the single-mode fiber core, the fiber tip acts as both a point source and a point detector, thereby facilitating confocal detection, i.e., only fluorescence from a small volume at the focal plane is collected. *Z* sectioning can be achieved by rotating a knob on the handle, which moves the entire scanning mechanism (including both magnetic coils and the tuning fork) axially along the tube. This provides a mechanical range of almost $300\ \mu\text{m}$ below the surface. A maximum power of $<0.5\ \text{mW}$ can be obtained at the surface of the tissue.

Synchronization between the electronic signals from the PMT and the sampling positions is provided by the main control unit (MCU), which communicates with a personal computer (PC) via a frame grabber card and a COM port. The frame grabber in the MCU outputs one frame of 512×512 pixels image per s to the PC. The pixel resolution in a 512×512 pixels image is $0.8\ \mu\text{m}$ per pixel.

2.2 Imaging with ALA in Human Subjects

A 0.4% solution of ALA was freshly prepared by dissolving 5-aminolevulinic acid hydrochloride (Medac, Germany) in phosphate buffered solution (PBS) with the pH adjusted to between 6.5 and 7.4. Three healthy volunteers and three patients with SCC of the tongue were recruited for the pilot study following informed consent. Topical application in the oral cavities of the subjects was achieved by 15 min of continuous rinsing under supervision, followed by an incubation period of at least 30 min. Imaging using the LCE was carried out between 30 to 120 min after administration of ALA. Excised tissue of the SCC tongue was sectioned and processed for hematoxylin and eosin (H&E) staining.

2.3 Imaging with ALA in Animal Models

Male Sprague-Dawley rats (4 to 6 weeks old) were used as animal models. The animals were anesthetized for survival procedures, and topical application was carried out by the insertion of cotton buds soaked in freshly prepared 0.4% ALA solution (preparation described in Sec. 2.2) into the oral cavity for 15 min, followed by an incubation period of 30 min. After the incubation period, the rats were sacrificed by an overdose of carbon dioxide, and the tongue and buccal cavity tissue were excised for imaging using the LCE. Images obtained using the LCE were compared to images obtained using a conventional benchtop confocal laser scanning microscope (Carl-Zeiss LSM Meta 510) operating with a 488-nm excitation source.

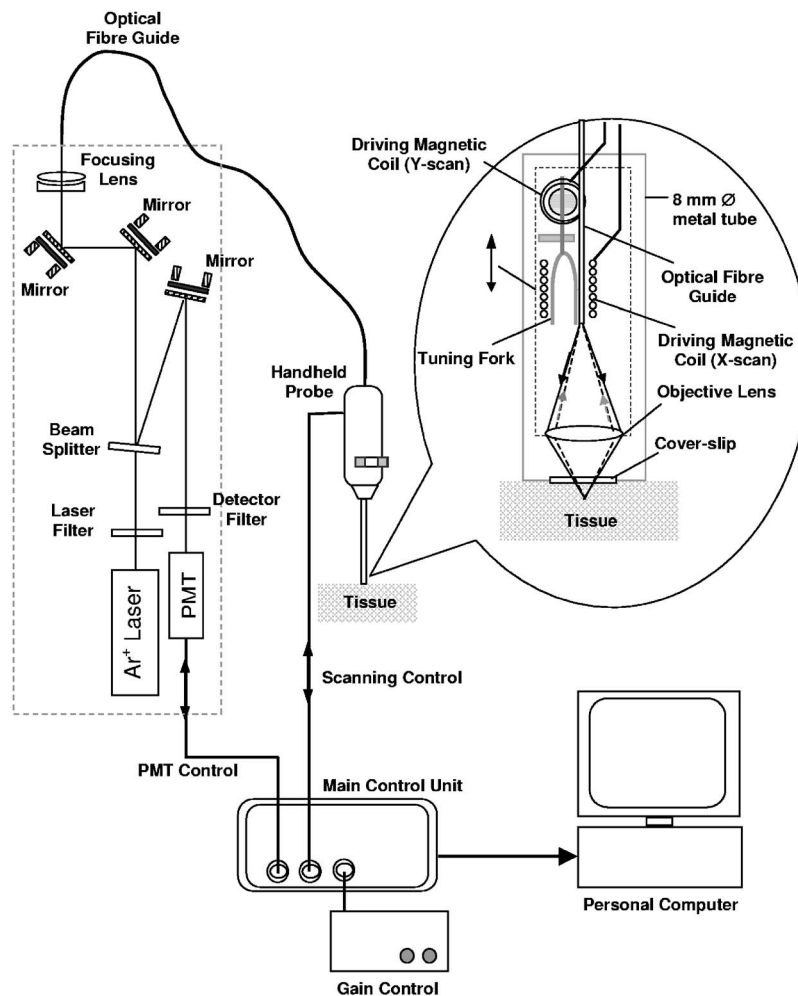


Fig. 1 Schematic diagram of the laser confocal endomicroscope (LCE) system with a handheld rigid probe that was used for fluorescence imaging of the oral cavity. The inset shows details within the probe tip containing the miniaturized scanning mechanism.

2.4 Imaging with Fluorescein Sodium in Animal Models

Fluorescein sodium was also used as a contrast agent in 4-to-6 week-old male Sprague-Dawley rat models. The animals were anesthetized for survival procedures, and topical application was carried out by the insertion of cotton buds soaked in freshly prepared 0.1% fluorescein sodium solution (Sigma-Aldrich) into the oral cavity for 15 min. The rats were then sacrificed by an overdose of carbon dioxide, and the tongue and buccal cavity tissue were excised for imaging.

2.5 Use of Pharmasolve in Animal Models

The pharmaceutical-grade solvent N-methyl-pyrrolidone, trade name Pharmasolve (ISP Technologies, Inc., Wayne, New Jersey), was used with 5-ALA and fluorescein sodium to enhance the penetration depths of these drugs in the oral cavity of animal models. A 5% solution of Pharmasolve was prepared in PBS and mixed with a solution of 0.4% ALA (prepared as described in Sec. 2.2). Topical application of the ALA-Pharmasolve solution was carried out in the rat oral cavity as described in Sec. 2.3. Likewise, a 5% Pharmasolve

solution was mixed with a 0.1% fluorescein sodium solution (preparation described in Sec. 2.3) and topically applied to the rat oral cavity as described in Sec. 2.4.

2.6 Carcinogen-Induced Model of Oral Cavity SCC

The water-soluble carcinogen 4-nitroquinoline-N-oxide (4-NQO) was used to induce a rat model of oral cavity SCC. 4-NQO (Sigma-Aldrich) was dissolved in acetone and diluted in water to make up a 0.002% solution. The 4-NQO solution was then fed to the rats as drinking water for 24 weeks. The rats were allowed to drink freely of the 4-NQO solution. After 24 weeks, a solution of 0.4% ALA and 5% Pharmasolve was prepared as described in Sec. 2.5 and topically applied to the oral cavity of the 4-NQO rats. Fluorescence imaging of the oral cavity was carried out after 30 min, as described in Sec. 2.3. The excised tissue was sectioned and processed for H&E staining.

3 Results and Discussion

3.1 Imaging the Human Oral Cavity

In a pilot study, ALA-induced PpIX fluorescence imaging of the human tongue was carried out in healthy volunteers and

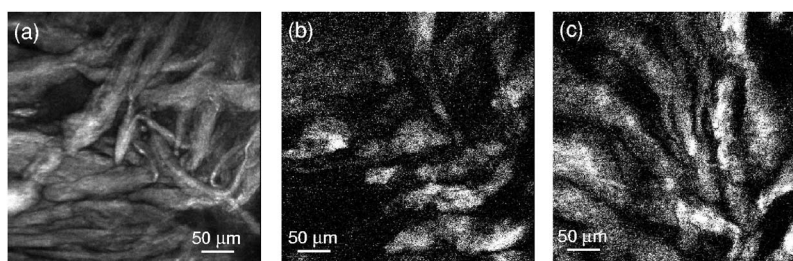


Fig. 2 ALA-induced PpIX fluorescence LCE images of a normal human tongue in a healthy volunteer. (a), (b), and (c) show images captured 45 min, 90 min, and 120 min after ALA administration, respectively. Clear images of the tongue could be obtained as early as 45 min after ALA administration. The scale bars in the images represent 50 μm in these images, with approximate fields of view of 390 $\mu\text{m} \times 390 \mu\text{m}$.

patients with malignant SCC lesions of the tongue. A 0.4% ALA solution was administered topically, and fluorescence imaging was carried out using the LCE after an incubation period of at least 30 min. Figure 2 shows ALA-induced PpIX fluorescence LCE images of a normal human tongue in a healthy volunteer. Figures 2(a)–2(c) show images captured 45 min, 90 min, and 120 min after ALA administration, respectively. Clear images of the tongue could be obtained as early as 45 min after ALA administration. Imaging after longer time periods of up to 120 min after ALA administration did not offer any advantage over imaging at an earlier time point. The images at later time points 90 min and 120 min carry more noise and are not as sharp as the image at 45 min. This is probably due to clearance of PpIX, leading to reduced fluorescence signals at later time points.

Figure 3(a) shows an ALA-induced PpIX fluorescence LCE image obtained from a patient with SCC of the tongue, while Fig. 3(b) shows a white light microscope image of an H&E-stained section of an SCC tongue. In image (b), the SCC region is characterized by dark nuclei (red arrows) and slightly less dark cytoplasm. The surrounding tissue has many inflammatory cells with smaller nuclei (black arrows). The fluorescence image in (a) shows small structures of similar size that are probably the inflammatory cells (white arrows). Larger structures (red arrows) represent the squamous epithelium of the SCC. Thus, LCE images of normal (Fig. 2) and SCC [Fig. 3(a)] tongues appear distinctly different, allowing us to distinguish between normal and lesion tissue using ALA-induced PpIX fluorescence imaging. This shows the potential of the LCE for diagnosis of oral cavity lesions such as SCC of the tongue.

3.2 Imaging the Rat Oral Cavity with ALA

ALA-induced PpIX fluorescence endomicroscopic imaging of the oral cavity was also carried out in rat models. ALA-induced PpIX fluorescence images of the dorsal surface of the normal rat tongue obtained using the LCE and a conventional CLSM 30 min after topical application of 0.4% ALA solution in the rat oral cavity are shown in Figs. 4(a) and 4(b), respectively. Fungiform papillae appear broad and round and are indicated by dotted white arrows in both images. Conical filiform papillae are more numerous and are indicated by solid white arrows in both images. Thus a comparison of (a) and (b) shows that the LCE can capture ALA-induced PpIX fluorescence images of structures on the rat tongue similar to those that can be obtained using a conventional benchtop CLSM.

3.3 Imaging the Rat Oral Cavity with Fluorescein Sodium

As a comparison, ALA-induced PpIX fluorescence images of the rat oral cavity were compared to fluorescence images obtained using fluorescein sodium, a fluorophore that is commonly used for fluorescence imaging. A 0.1% fluorescein solution was topically applied in the rat oral cavity. The tongue and buccal tissue in the rat oral cavity were imaged using the LCE after an incubation period of at least 30 min. Figure 5(a) shows an LCE fluorescence image of the dorsal surface of the rat tongue. Filiform papillae (dotted white arrows) can be easily identified in this image. These structures are similar to those observed in the ALA-induced PpIX fluorescence image of the rat tongue obtained after ALA application, shown in Fig. 4(a). Fluorescence images of the surface of the rat buccal tissue obtained after topical application of fluorescein using the LCE (b) and a conventional benchtop CLSM (c) both show squamous epithelial cells of the surface of the mucosa (solid white arrows in both). These are the mature mucosal squamous cells at the surface of the buccal epithelium. They form a flat pavement-like surface with distinct cell boundaries that is typical of the surface of squamous mucosa.

3.4 Use of Pharmasolve in Animal Models

The pharmaceutical-grade solvent Pharmasolve was used with ALA and fluorescein in rat models to enhance the penetration of these drugs in the rat oral cavity. Pharmasolve was mixed with solutions of 0.4% ALA or 0.1% fluorescein sodium, and the solution mixture was topically applied to the rat oral cavity. Fluorescence imaging of the rat oral cavity was carried out using the LCE after an incubation period of at least 30 min. Figure 6(a) shows the fluorescence image of rat buccal mucosa obtained at the surface of the tissue after topical application of a mixture of fluorescein sodium and Pharmasolve. Figure 6(b) shows an image of the same tissue area obtained at a subsurface depth of about 60 μm , indicating that fluorescein, when mixed with Pharmasolve, penetrated about 60 μm into the buccal mucosa. By comparison, in rats that received topical application of fluorescein alone, no images of the buccal mucosa can be obtained below the surface. Thus, the use of Pharmasolve enhanced the penetration depth of fluorescein in the rat buccal mucosa.

Preliminary experiments on the rat tongue were also carried out to estimate the maximum subsurface depth from which images can be obtained after topical application of ALA and fluorescein sodium with and without the addition of

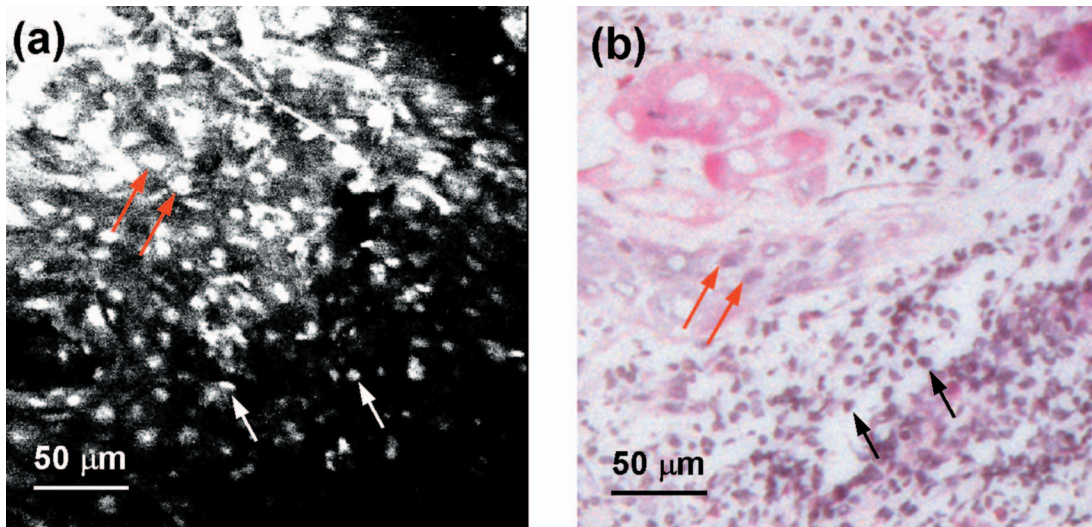


Fig. 3 (a) An ALA-induced PpIX fluorescence LCE image obtained from a patient with SCC of the tongue. (b) A white light microscope image of a hematoxylin and eosin (H&E) stained section of a human SCC tongue. In (b), the SCC region is characterized by dark nuclei ([red] arrows) and slightly less dark cytoplasm. The surrounding tissue has many inflammatory cells with smaller nuclei (black arrows). The fluorescence image in (a) shows small structures of similar size that are probably the inflammatory cells (white arrows). Larger structures ([red] arrows) represent the squamous epithelium of the SCC.

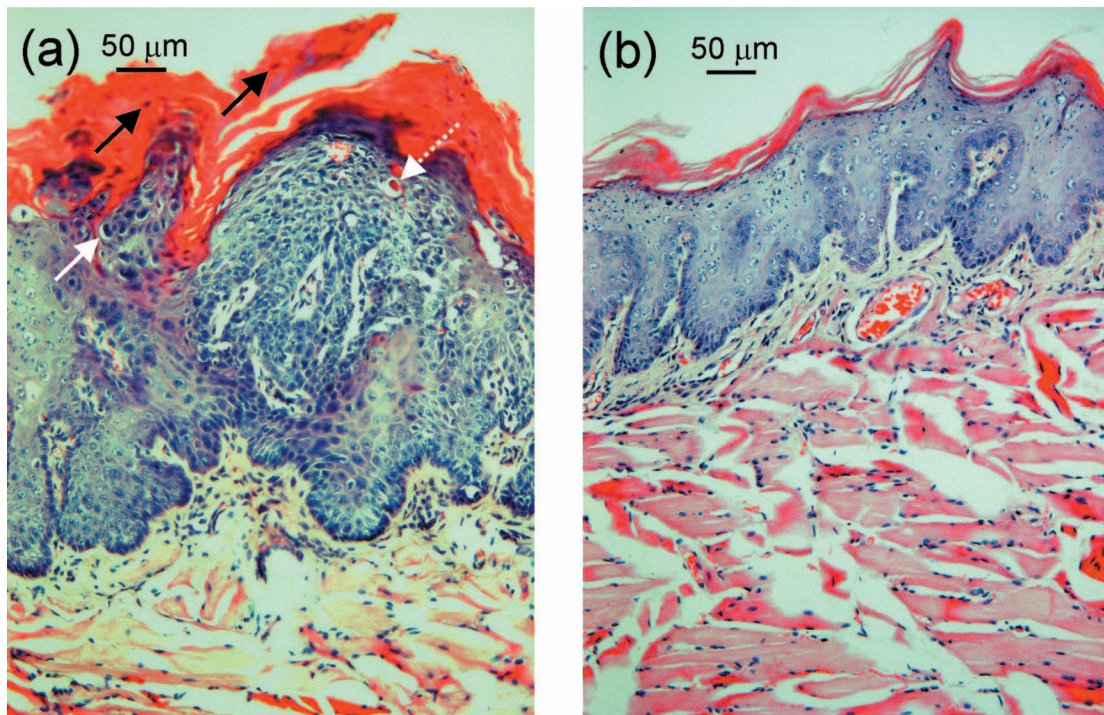


Fig. 8 (a) A dysplastic region within an H&E stained section of a 4-NQO carcinogen-induced SCC rat tongue. (b) An adjacent normal region within the same specimen. The dysplastic region is characterized by a thicker, proliferating epithelium. The proliferating keratinocytes have scant cytoplasm and relatively large nuclei that are hyperchromatic, with prominent nucleoli. Perinuclear vacuolation is noted around a few of the larger dysplastic nuclei (white solid arrow). Some necrotic dysplastic cells are present, with eosinophilic cytoplasm (white dotted arrow). Dysplastic nuclei appear in the most superficial thickened layer (black arrows). All of these features are lacking in the normal region in (b).

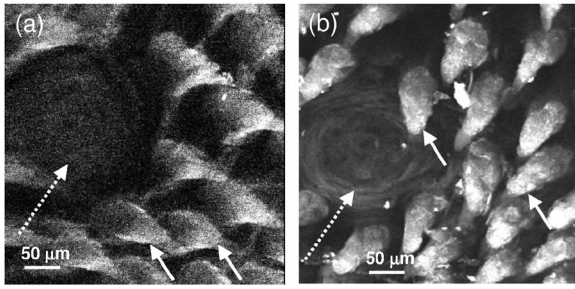


Fig. 4 ALA-induced PpIX fluorescence images of the dorsal surface of the normal rat tongue obtained 30 min after topical application of 0.4% ALA solution in the rat oral cavity obtained using the LCE (a) and a conventional benchtop CLSM (b). Fungiform papillae appear broad and round and are indicated by dotted white arrows in both images. Conical filiform papillae are more numerous and are indicated by solid arrows in both images.

Pharmasolve. This maximum depth was estimated by turning the focusing knob to focus in increasingly deeper layers below the tissue surface until no discernible features can be obtained in the image. The depth estimates showed that the use of Pharmasolve with ALA increased the maximum image depth on the rat tongue by up to 80 μm , from 195 μm without to 275 μm with Pharmasolve. Thus, our preliminary results show that the use of Pharmasolve with ALA and fluorescein enhanced the penetration depths of both drugs and enabled us to obtain images from deeper layers of the tissue in animal models.

3.5 Carcinogen-Induced Model of SCC

The water-soluble carcinogen 4-NQO was used to induce a rat model of oral cavity SCC. After 24 weeks, a small white patch was observed in the tongue of the rat, resembling early SCC of the tongue. Prior to imaging the SCC tongue, a solution mixture of 0.1% fluorescein and 5% Pharmasolve was topically applied to the oral cavity of the rat, followed by 30 min of incubation. Figure 7(a) shows an LCE fluorescence image of the SCC rat tongue. This image shows disorganized structures in the SCC rat tongue. In contrast, Fig. 7(b) shows the fluorescence image taken of a normal (non-SCC) rat tongue also with a topically applied mixture solution of 0.1% fluorescein and 5% Pharmasolve. This image shows the same organized structures of filiform papillae as were observed in

fluorescence images of the normal rat tongue obtained using ALA [Fig. 4(a)] and fluorescein [Fig. 5(a)]. Thus, we are able to observe morphological differences between the normal and SCC rat tongues from fluorescence images obtained using the LCE.

Tissue from the SCC rat tongue was also processed for H&E staining to provide histological characterization. Figure 8(a) shows a dysplastic region within an H&E stained section of the SCC rat tongue. Figure 8(b) shows an adjacent normal region within the same specimen. The dysplastic region is characterized by a thicker, proliferating epithelium. The proliferating keratinocytes have scant cytoplasm and relatively large nuclei that are hyperchromatic, with prominent nucleoli. Perinuclear vacuolation is noted around a few of the larger dysplastic nuclei (white solid arrow). Some necrotic dysplastic cells are present, with eosinophilic cytoplasm (white dotted arrow). Dysplastic nuclei appear in the most superficial thickened layer (black arrows). All of these features are lacking in the normal region in (b).

4 Conclusion

Early detection is crucial for a good prognosis of oral cancers. However tumors of the oral cavity are often flat or superficial, making it difficult to distinguish between benign and premalignant or early lesions. Histopathological examination of biopsy tissue remains the gold standard for the diagnosis of oral cavity malignancies. The process is time consuming, and patients bear the risk of complications arising from the biopsy procedure. Previous work by our group has shown the superiority of fluorescence endoscopic imaging of ALA-induced PpIX fluorescence at the macroscopic level over white light endoscopy in the diagnosis of oral cancers.^{10,13} In this pilot study, we investigated the use of a prototype laser confocal endomicroscope (LCE) with a handheld rigid probe as an optical imaging technique for noninvasive fluorescence diagnostic imaging of the oral cavity at the microscopic level.

ALA-induced PpIX fluorescence endomicroscopic imaging of the human tongue was carried out in healthy volunteers and patients with malignant SCC lesions of the tongue following topical application of ALA. Good images of the tongue could be obtained as early as 45 min after ALA. Thus, ALA-induced PpIX fluorescence diagnosis using the LCE can be completed within a reasonably short time and minimizes waiting time for both patients and clinicians.

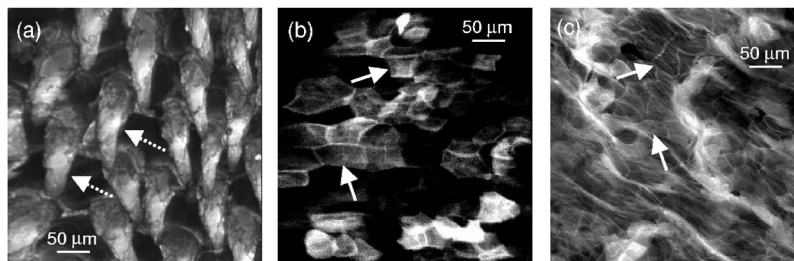


Fig. 5 (a) An LCE fluorescence image of the dorsal surface of the rat tongue obtained 30 min after topical application of fluorescein. Filiform papillae (dotted white arrows) can be identified, similar to those observed in Fig. 4(a). Fluorescence images of the surface of the rat buccal tissue obtained after topical application of fluorescein using the LCE (b) and a conventional benchtop CLSM (c) both show squamous epithelial cells of the surface of the mucosa (solid white arrows in both). These are the mature mucosal squamous cells at the surface of the buccal epithelium. They form a flat pavement-like surface with distinct cell boundaries that is typical of the surface of squamous mucosa.

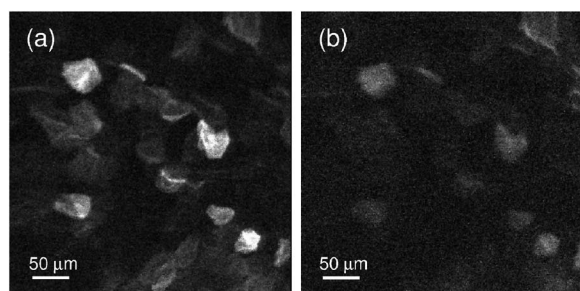


Fig. 6 LCE fluorescence images of the rat buccal mucosa obtained at the surface of the tissue (a) and at a subsurface depth of about $60\ \mu\text{m}$ (b) after topical application of a solution mixture of fluorescein and Pharmasolve.

Using the LCE, we were able to capture fluorescence images of the human SCC tongue showing cellular structures similar in size to those seen in an H&E-stained section of the SCC tongue. LCE images of normal and SCC tongues appear distinctly different, allowing us to distinguish between normal and lesion tissue using ALA-induced PpIX fluorescence imaging. This shows the potential of the LCE for fluorescence diagnosis of oral cavity malignancies such as SCC of the tongue.

ALA-induced PpIX fluorescence endomicroscopic imaging of the oral cavity was also carried out in rat models following topical application of ALA. Fluorescence images showed identifiable morphological structures on the rat tongue, such as filiform and fungiform papillae, that can be distinguished clearly and that were similar to structures that can be visualized using a conventional benchtop CLSM.

As a further comparison, ALA-induced PpIX fluorescence images of the rat oral cavity were compared to fluorescence images obtained using fluorescein sodium, a fluorophore that is commonly used for fluorescence imaging. LCE fluorescence images of the rat tongue showed filiform papillae similar to those observed in ALA-induced PpIX fluorescence images. LCE images of the rat buccal mucosa showed squamous epithelial cells on the surface of the mucosa similar to those visualized using a conventional CLSM.

Although the mechanical range of the rigid probe is approximately $300\ \mu\text{m}$, the actual imaging depth depends on tissue optics, penetration depth of the fluorescent dye, etc. We explored the efficacy of the pharmaceutical-grade solvent Pharmasolve as a penetration enhancer of ALA and fluorescein in the oral cavity in rat models. Our preliminary results showed that the use of Pharmasolve enhanced the penetration depths of both drugs in the rat oral cavity and enabled us to obtain images from deeper layers of the tissue.

Finally, the water-soluble carcinogen 4-NQO was used to induce a rat model of oral cavity SCC. Fluorescence endomicroscopic imaging of the SCC rat tongue using the LCE showed disorganized structures, in contrast to images of a normal rat tongue showing organized structures, allowing us to distinguish between normal and SCC rat tongues.

In summary, a confocal fluorescence endomicroscope with a rigid probe can provide good structural imaging of the oral cavity. Morphological differences between normal and lesion tongue tissue can be distinguished using ALA-induced PpIX fluorescence. The penetration depth of ALA can be enhanced

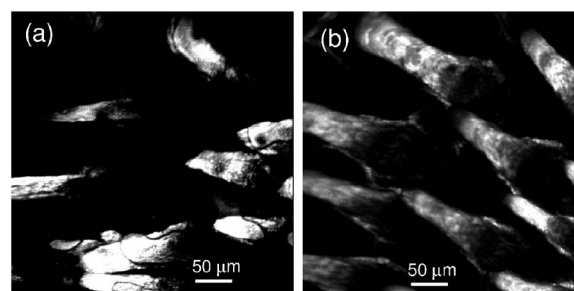


Fig. 7 (a) An LCE fluorescence image of a 4-NQO carcinogen-induced SCC rat tongue after topical application of a mixture of fluorescein and Pharmasolve. Disorganized structures are observed in the SCC rat tongue. In contrast, (b) shows the fluorescence image taken of a normal rat tongue also with a mixture solution of fluorescein and Pharmasolve topically applied. This image shows the same organized structures of filiform papillae as were observed in fluorescence images of the normal rat tongue obtained using ALA [Fig. 4(a)] and fluorescein [Fig. 5(a)]. Thus, LCE fluorescence imaging allows us to distinguish morphological differences between the normal and the SCC rat tongues.

by using the pharmaceutical-grade solvent Pharmasolve so that fluorescence endomicroscopic images can be obtained from deeper layers within the oral cavity tissue. Our results show that laser confocal fluorescence endomicroscopy has the potential to be used as a noninvasive optical biopsy method for early diagnosis of oral cavity malignancies.

Acknowledgments

The authors thank the Biomedical Research Council (Singapore) for funding this project, Optiscan Imaging Pty. Ltd. (Australia) for the loan of the instrument to the National Cancer Centre (Singapore), and Ms. Vanaja Manivasager and Ms. Bhuvana Ramaswamy for assistance.

References

1. N. Johnson, "Tobacco use and oral cancer: a global perspective," *J. Dent. Educ.* **65**(4), 328–339 (2001).
2. S. Warnakulasuriya, G. Sutherland, and C. Scully, "Tobacco, oral cancer, and treatment of dependence," *Oral Oncol.* **41**(3), 244–260 (2005).
3. R. Kiesslich and M. F. Neurath, "Endoscopic confocal imaging," *Clin. Gastroenterol. Hepatol.* **3**(7 Suppl. 1), S58–S60 (2005).
4. J. A. Evans and N. S. Nishioka, "Endoscopic confocal microscopy," *Curr. Opin. Gastroenterol.* **21**(5), 578–584 (2005).
5. W. J. McLaren, P. Anikijenko, S. G. Thomas, P. M. Delaney, and R. G. King, "In vivo detection of morphological and microvascular changes of the colon in association with colitis using fiberoptic confocal imaging (FOCI)," *Dig. Dis. Sci.* **47**(11), 2424–2433 (2002).
6. R. Kiesslich, J. Burg, M. Vieth, J. Gnaendiger, M. Enders, P. Delaney, A. Polglase, W. McLaren, D. Janell, S. Thomas, B. Nafe, P. R. Galle, and M. F. Neurath, "Confocal laser endoscopy for diagnosing intraepithelial neoplasias and colorectal cancer in vivo," *Gastroenterology* **127**(3), 706–713 (2004).
7. A. L. Polglase, W. J. McLaren, S. A. Skinner, R. Kiesslich, M. F. Neurath, and P. M. Delaney, "A fluorescence confocal endomicroscope for in vivo microscopy of the upper- and the lower-GI tract," *Gastrointest. Endosc.* **62**(5), 686–695 (2005).
8. S. Collaud, A. Juzeniene, J. Moan, and N. Lange, "On the selectivity of 5-aminolevulinic acid-induced protoporphyrin IX formation," *Curr. Med. Chem.* **4**(3), 301–316 (2004).
9. C. S. Betz, H. Stepp, P. Janda, S. Arbogast, G. Grevers, R. Baumgartner, and A. Leunig, "A comparative study of normal inspection, autofluorescence and 5-ALA-induced PpIX fluorescence for oral cancer diagnosis," *Int. J. Cancer* **97**(2), 245–252 (2002).

10. W. Zheng, K. C. Soo, R. Sivanandan, and M. Olivo, "Detection of squamous cell carcinoma and pre-cancerous lesions in the oral cavity by quantification of 5-aminolevulinic acid induced fluorescence endoscopic images," *Lasers Surg. Med.* **31**(3), 151–157 (2002).
11. H. Messmann, E. Endlicher, G. Freunek, P. Rummele, J. Scholmerich, and R. Knuchel, "Fluorescence endoscopy for the detection of low and high grade dysplasia in ulcerative colitis using systemic or local 5-aminolevulinic acid sensitisation," *Gut* **52**(7), 1003–1007 (2003).
12. M. Csanady, J. G. Kiss, L. Ivan, J. Jori, and J. Czigner, "ALA (5-aminolevulinic acid)-induced protoporphyrin IX fluorescence in the endoscopic diagnostic and control of pharyngo-laryngeal cancer," *Eur. Arch. Otorhinolaryngol.* **261**(5), 262–266 (2004).
13. W. Zheng, K. C. Soo, and M. Olivo, "The use of digitized endoscopic imaging of 5-ALA-induced PPIX fluorescence to detect and diagnose oral premalignant and malignant lesions in vivo," *Int. J. Cancer* **110**(2), 295–300 (2004).
14. W. Zheng, M. Harris, K. W. Kho, P. S. P. Thong, A. Hibbs, M. Olivo, and K. C. Soo, "Confocal endomicroscopic imaging of normal and neoplastic human tongue tissue using ALA-induced-PPIX fluorescence: a preliminary study," *Oncol. Rep.* **12**(2), 397–401 (2004).
15. T. Ogiso, T. Paku, M. Iwaki, and T. Tanino, "Percutaneous penetration of fluorescein isothiocyanate-dextran and the mechanism for enhancement effect of enhancers on the intercellular penetration," *Biol. Pharm. Bull.* **18**(11), 1566–1571 (1995).